Food Chemistry 119 (2010) 1285–1292

Contents lists available at ScienceDirect

Food Chemistry

journal homepage: www.elsevier.com/locate/foodchem

Bioassay-guided isolation and EPR-assisted antioxidant evaluation of two valuable compounds from mango peels

L.Y. Jiang [a], S. He [b], Y.J. Pan [a], C.R. Sun [a,*]

[a] Department of Chemistry, Zhejiang University, Hangzhou 310027, China
[b] Institute of Biological Chemistry, Washington State University, Pullman, WA 99164-6340, USA

ARTICLE INFO

Article history:
Received 2 April 2009
Received in revised form 8 July 2009
Accepted 2 September 2009

Keywords:
Antioxidant
Mango peels
HPLC/ESI-MS^2
Ethyl gallate
Penta-*O*-galloyl-glucoside
Hydroxyl radical
Synergistic effects
Superoxide anion
Singlet oxygen
EPR
Spin-trapping

ABSTRACT

Bioassay-guided HPLC/ESI-MS^2 analysis of the ethyl acetate extract of mango peels (MPE) led to the isolation of two major valuable compounds, ethyl gallate (**2**) and penta-*O*-galloyl-glucoside (**5**). In this work, EPR spin-trapping technique was utilised for their antioxidant evaluation on the level of reactive oxygen species. Results demonstrated MPE, **2** and **5** possessed potent scavenging effects on hydroxyl radicals (·OH), superoxide anions ($O_2^{\cdot-}$) and singlet oxygen ($^1O_2$). With respect to ·OH, **5** has much stronger inhibitory activity than **2,** owing to more galloyl groups and the occurrence of intramolecular reactions in **5**. Synergistic effects could be observed and explained the strongest scavenging property of MPE (IC_{50} = 4.08 μg/ml, $k_A = 3.51 \times 10^{15}\ M^{-1}\ S^{-1}$) in terms of more potent inhibition of **5,** which was caused by the inhibitory effects of **2** on **5** consumption. Regarding $^1O_2$, **2** has a stronger quenching activity than **5**, partially revealing that gallate type compounds quenched $^1O_2$ with different mechanisms from those proposed against ·OH.

1. Introduction

Reactive oxygen species (ROS) are by-products of normal cellular metabolism in aerobic life where molecular oxygen is ubiquitous. Due to the disturbance in the equilibrium state of prooxidant/antioxidant reaction, ROS are overproduced to induce oxidative stress that inhibits normal functions of cellular lipids, proteins, DNA and RNA. Three most typical species of ROS are hydroxyl radical (·OH), superoxide anion ($O_2^{\cdot-}$) and singlet oxygen ($^1O_2$). ·OH is highly reactive with a very short half-life of about 10^{-9} s *in vivo* (Pastor, Weinstein, Jamison, & Brenowitz, 2000) and thus it is a very dangerous species of oxygen metabolite generated in living organisms. $O_2^{\cdot-}$ could easily damage cells (Halliwell, 1974), either by direct reaction with cellular components or indirect production of ·OH and $^1O_2$. $^1O_2$, which is an excited form of molecular oxygen obtained *via* either photoirradiated oxidation or other non-light-mediated processes, can cause physical harm to a wide range of biological substances (Ravanat, Mascio, Martinez, Medeiros, & Cadet, 2000; Vile & Tyrrell, 1995). It is evident that these harmful consequences appear to be associated with various diseases, such as cancer, cardiovascular diseases, ischaemic injury, multiple sclerosis, rheumatoid arthritis, diabetes, neurological disorders and senescence (Mark, 1987; Valko et al., 2007). Hence, to search for antioxidants regarded as those substances, which will significantly delay or inhibit oxidation of oxidisable substrates at low concentrations compared to those of desired substrates, is of great interest in the scientific community.

Mango (*Mangifera indica* L.), belonging to the family Anacardiaceae, the order Rutales, is one of the most popular edible fruits and its production, at present, ranks 5th in the world among major fruit crops (Ajila, Bhat, & Rao, 2007). During juice and canned mango manufacture, mango peels that account for 15–20% weight of the whole fruit (Beerh, Raghuramaiah, Krishnamurthy, & Giridhar, 1976) are generated as by-products. Mango peels have not been used for any commercial purposes, so they are discarded as waste and cause serious pollution. However, mango peels have been reported to be rich sources of gallates, gallotannins, xanthone glucosides, flavonols (Barreto et al., 2008; Ribeiro, Barbosa, Queiroz, Knödler, & Schieber, 2008), ascorbic acid, carotenoids, enzymes and dietary fibre (Frenich, Torres, Vega, Vidal, & Bolaos, 2005; Ajila et al., 2007). Pharmaceutical studies have been performed, indicating that gallate type compounds, for example penta-*O*-galloyl-glucoside, have various bioactivities, including antioxidant (Hatano

* Corresponding author. Tel.: +86 571 87953000; fax: +86 571 87951629.
E-mail address: suncuirong@zju.edu.cn (C.R. Sun).

0308-8146/$ - see front matter © 2009 Elsevier Ltd. All rights reserved.
doi:10.1016/j.foodchem.2009.09.005

et al., 1989), antitumour (Lizarraga et al., 2008), hepatoprotective (Eun-Jeon, Zhao, Ren-Bo, Youn-Chui, & Hwan, 2008), and anticardiovascular effects (Ignarro, Balestrieri, & Napoli, 2007).

Electron paramagnetic resonance (EPR) spectroscopy, whose signal intensities depend on the concentrations of free radicals, is a very powerful and useful analytical technique for the detection of radical species including ROS in chemical, physical and biological systems. The method in which active oxygen radicals with very short half-lives are trapped by a proper trapper, yielding much more stable radical-trapper adducts with characteristic EPR spectra, is termed as EPR spin-trapping technique, which eliminates the disadvantages caused by traditional methods, such as low reliability, precision and delicacy. The technique has been successfully applied for systematic studies about the evaluation of antioxidant capacities of foods, such as apple pomace (Ćerković et al., 2008) and wheat extracts (Yu, Haley, Perret, & Harris, 2002).

Therefore, to develop new potential application of mango peels and reduce their environmental pollution, the investigation of antioxidant capacities on ROS levels of mango peels and their major components has been performed using EPR spin-trapping technique.

2. Materials and methods

2.1. Materials

The cultivar of mango studied here was Carabao bought from a local market in Hangzhou, China. Peels were collected by a sharp knife and the underlying pulp was discarded by gently scraping with its blunt edge. The fresh peels were used for the subsequent studies.

5,5-Dimethyl-1-pyrroline-*N*-oxide (DMPO), 2,2,6,6-tetramethylpiperidine (TEMP), rose Bengal and riboflavin were purchased from Sigma, St. Louis, MO. The DMPO (900 mM) solution was purified as follows: stirred with activated charcoal at 10 mg/ml; membrane-filtered (0.45 μm); centrifuged at 2000 *g* for 2 min. No additional EPR signals were observed in the purified DMPO solution. Deionised water (18 MΩ) was obtained from a Milli-Q water purification system (Millipore, Bedford, MA). Acetonitrile used for analytical and preparative HPLC was of chromatographic grade and purchased from Merck, Darmstadt, Germany. All the other chemicals, including hydrogen peroxide (H_2O_2), ferrous sulfate ($FeSO_4$), ethylenediaminetetraacetic acid (EDTA), acetic acid and acetone, were obtained at the highest available purity in China.

2.2. Identification and quantification of two valuable compounds

2.2.1. Sample preparation

The air-dried mango peels (2 g) were chipped and extracted three times with 250 ml 95% ethanol under reflux, yielding an ethanol extract (1 g). Then, an aqueous solution of the ethanol extract (1 g) was extracted with 100 ml ethyl acetate for four times. Extracts were combined and evaporated under reduced pressure at 40 °C to obtain the ethyl acetate extract of mango peels named MPE (0.43 g). MPE was stored in a refrigerator (4 °C); it was dissolved in mobile phase (1 mg/ml), membrane-filtered (0.45 μm), and analysed by HPLC/ESI-MS^2.

MPE was separated by preparative HPLC, using a gradient elution which started at 19% acetonitrile and linearly increased to 21% acetonitrile in 30 min at room temperature, to obtain compound **2** (4.3 mg) and compound **5** (5.1 mg), with purities of 98% and 96%, respectively. The flow rate was 8.0 ml/min and the detector wavelength was 280 nm. A Varian Workstation equipped with a Varian PrepStar binpump and a Varian ProStar variable-wavelength detector (Varian Co., Palo Alto, CA) was used. A Shimadzu (Kyoto, Japan) reversed-phase Shim-pack PRC ODS (20 × 250 mm, 10 μm) was used.

2.2.2. HPLC/ESI-MS^2 analysis

An Agilent 1100 system, including a G1311A quaternary pump, a G1322 degasser, a G1314A variable wave detector (VWD), a model 7725i injection valve with a 20 μl loop and an Agilent ChemStation for LC, was employed (Agilent, Santa Clara, CA). Samples were analysed on a Hypersil BDS reversed-phase C18 column (4.6 mm × 250 mm i.d., 5 μm; Thermo Scientific, Waltham, MA) with a flow rate of 1.0 ml/min at room temperature. Good chromatograms recorded at 280 nm were obtained, using a linear gradient elution of 2% acetic acid in water (**A**) and acetonitrile (**B**) with the gradient procedure as follows: 0 min, **B** 10%; 20 min, **B** 16%; 45 min, **B** 17%.

HPLC/ESI-MS^2 experiments were performed on the above HPLC system coupled with a Bruker Esquire 3000^{plus} ion trap mass spectrometer (Bruker-Franzen Analytik GmbH, Bremen, Germany). The mass spectrometer was equipped with an electrospray ionisation (ESI) interface. The LC effluent was induced into the ESI source with a T-junction in a splitting ratio of 2:1. Precursor ions were produced in the negative ion mode for the compounds of interest. Data acquisition was performed using Esquire 5.0 software. Other scan conditions were set as follows: fragmentation amplitude, 1.0 V; needle voltage, 4000 V; nebuliser pressure, 30 psi; ion source temperature, 250 °C; mass scan range, *m/z* 50–2000.

2.2.3. NMR spectroscopy

NMR analyses of **2** and **5** were carried out on a Bruker Avance DMX 500NMR spectrometer with acetone-d_6 as solvent and TMS as internal standard.

2.2.4. Quantification of two valuable compounds

Compounds **2** and **5** obtained by preparative HPLC were used as the standards for quantification. Herein an external standard method has been developed. Stock solutions (1.58 mg/ml for compound **2**, 1.88 mg/ml for compound **5**) were prepared by dissolving standards in methanol. Then by dilution of the stock solutions, diverse concentrations for calibration were obtained. Peak areas in HPLC chromatograms were plotted against concentrations of the standards. Therefore, based on the calibration curves, the amounts of the compounds in extracts were determined by the equations generated *via* linear regression.

2.3. EPR measurements

2.3.1. Hydroxyl radical (·*OH*) assay

A Fenton-type reaction was employed to generate ·OH and the radicals were detected as DMPO–OH adducts (He, Jiang, Wu, Pan, & Sun, 2009). The reaction mixture consisted of 25 mM H_2O_2, 250 μM $FeSO_4$, 50 mM purified DMPO and various concentrations of antioxidants freshly dissolved in acetone. Individual samples were transferred to a quartz capillary and fitted into the cavity of a Bruker A300 X-band EPR spectrometer, then recorded immediately. Some samples for kinetic studies were monitored for 60 min and recorded every 1 min. Relative EPR parameters as well as the calculation methods were the same as previously described (He et al., 2009).

2.3.2. Superoxide anion ($O_2^{\cdot-}$) assay

Generation of $O_2^{\cdot-}$ was achieved by the photoirradiated riboflavin/EDTA system (He et al., 2009) with some minor modifications. The reaction mixture contained the following reagents at their final concentrations: 0.3 mM riboflavin, 5.0 mM EDTA, 50 mM purified DMPO and antioxidants at various concentrations. After samples were transferred to a quartz capillary and placed in the EPR cavity,

the mixture was irradiated by an Hg lamp (power 100 W) at room temperature for 30 s and corresponding EPR spectra were recorded immediately with UV light on. The conditions of EPR measurement were the same as above, except for microwave power at 40.20 mW.

2.3.3. Singlet oxygen ($^1O_2$) assay

Singlet oxygen ($^1O_2$) was formed by photoirradiated rose Bengal (RB) in the presence of dissolved air and detected as TEMP-$^1O_2$ adducts (TEMPO) with TEMP as a trapper (He et al., 2009). Samples consisted of 18 μM RB, 23 mM TEMP and various concentrations of antioxidants, which were irradiated with an Hg lamp (power 100 W) for 2 min. Then respective EPR spectra were instantly recorded. Scan conditions were also the same as above, apart from microwave power at 15.98 mW and time constant at 10.24 ms.

3. Results and discussion

3.1. Identification and quantification

Preliminary EPR studies revealed that the ethyl acetate extract of mango peels (MPE) possessed powerful antioxidant activities. Compared to the individual control, 5.45 μg/ml MPE showed 60.5%, 69.8% and 41.9% inhibition of hydroxyl radicals (·OH), superoxide anions ($O_2^{\cdot-}$) and singlet oxygen ($^1O_2$), respectively. These phenomena motivated us to further investigate the details of MPE. Thus the analysis on the chemical composition of MPE was necessary (Fig. 1). According to their HPLC retention time, the main components of MPE were designated as **1** through **9**. To our best knowledge, precursor ions of the individual compounds from mango have been observed in the negative mode (Barreto et al., 2008); so the $[M–H]^-$ ions were discussed here with regard to their MS^2 fragmentations in subsequent studies.

ESI-MS^2 analysis in combination with the reference (Barreto et al., 2008) resulted in the structural determination of compounds **1**–**9** summarised in Table 1. Among them, **2** and **5** were the major components of MPE and their isolation was proposed. Compound **2** had a molecular weight of 198; the loss of 28 Da from *m/z* 197 to *m/z* 169 could be ascribable to the neutral loss of ethylene, which supported the presence of an ethyl group attached directly to the ester instead of two methyl groups. The structure (Fig. 1) was unambiguously identified as ethyl gallate by the analysis of NMR data. ^1H NMR (500 MHz, acetone-d_6): 7.10 (2H, s, H-2 and 5), 4.24 (2H, q, H-8), 1.31 (3H, t, H-9). ^{13}C NMR (125 MHz, acetone-d_6): 166.8 (C-7), 146.2 (C-3 and 5), 139.1 (C-4), 121.9 (C-1), 109.8 (C-2 and 6), 60.8 (C-8), 14.6 (C-9).

Table 1
Proposed assignments of compounds **1**–**9** shown in Fig. 1.

Compound number	Precursor ions $[M–H]^-$ (*m/z*)	Number of galloyl groups	Dominant fragment ions (*m/z*)
1	321	2	169, 125
2	197	1	169, 125
3	393	2	317, 169, 125
4	349	2	197, 169, 125
5	939	5	787, 769, 617
6	1091	6	939, 787, 769, 617
7	1091	6	939, 787, 769, 617
8	349	2	197, 169, 125
9	1091	6	939, 787, 769, 617

For compound **5**, the $[M–H]^-$ ion at *m/z* 939 eliminated fragments of 152 Da from *m/z* 939 to *m/z* 787 and 170 Da from *m/z* 939 to *m/z* 769, which were assigned as the loss of galloyl and gallic acid moieties respectively, indicating a fragmentation pattern typical of penta-*O*-galloyl-glucoside (Barreto et al., 2008). The structure of **5** (Fig. 1) was also confirmed by NMR data (Haddock, Gupta, Al-Shafi, & Haslam, 1982). ^1H NMR (500 MHz, acetone-d_6): 7.17, 7.10, 7.05, 7.00, and 6.97 (each 2H, s, galloyl H), 6.33 (1H, d, H-1, J = 9.5 Hz), 6.03 (1H, t, H-3, J = 9.5 Hz), 5.66 (1H, t, H-4, J = 9.5 Hz), 5.61 (1H, t, H-2, J = 9.5 Hz), 4.50 (1H, m, H-5), 4.50 (1H, m, H-6a), 4.41 (1H, dd, H-6b, J = 3.0 and 12.0 Hz). ^{13}C NMR (125 MHz, acetone-d_6): 93.4 (β-D-glucopyranose carbon atoms, C-1), 74.0 (β-D-glucopyranose carbon atoms, C-5), 73.3 (β-D-glucopyranose carbon atoms, C-3), 71.8 (β-D-glucopyranose carbon atoms, C-2), 69.4 (β-D-glucopyranose carbon atoms, C-4), 62.9 (β-D-glucopyranose carbon atoms, C-6), 166.4, 165.9, 165.7, 165.6, 165.0 (galloyl carbonyl carbon atoms).

Furthermore, other compounds were deduced as shown in Table 1. Identical molecular weights and fragment ions were observed for compounds **6**, **7** and **9** (Nishizawa et al., 1983) as well as **4** and **8**, which was attributed to the gallic acid substituted at different positions through the dehydration of two identical gallic acids.

Using the external standard method with the calibration curves (y = 0.0162x − 0.0496, r^2 = 0.9996 for **2**; y = 0.0497x + 0.2553, r^2 =

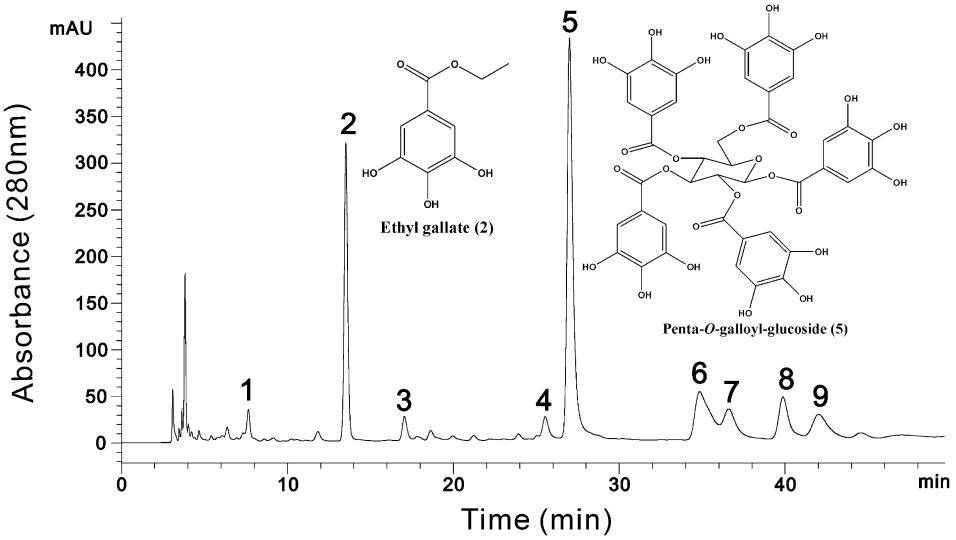

Fig. 1. Analytical HPLC analysis of the ethyl acetate extract of mango peels (MPE) and chemical structures of ethyl gallate (**2**) and penta-*O*-galloyl-glucoside (**5**). Peaks **1**–**9** were tentatively assigned in Table 1.

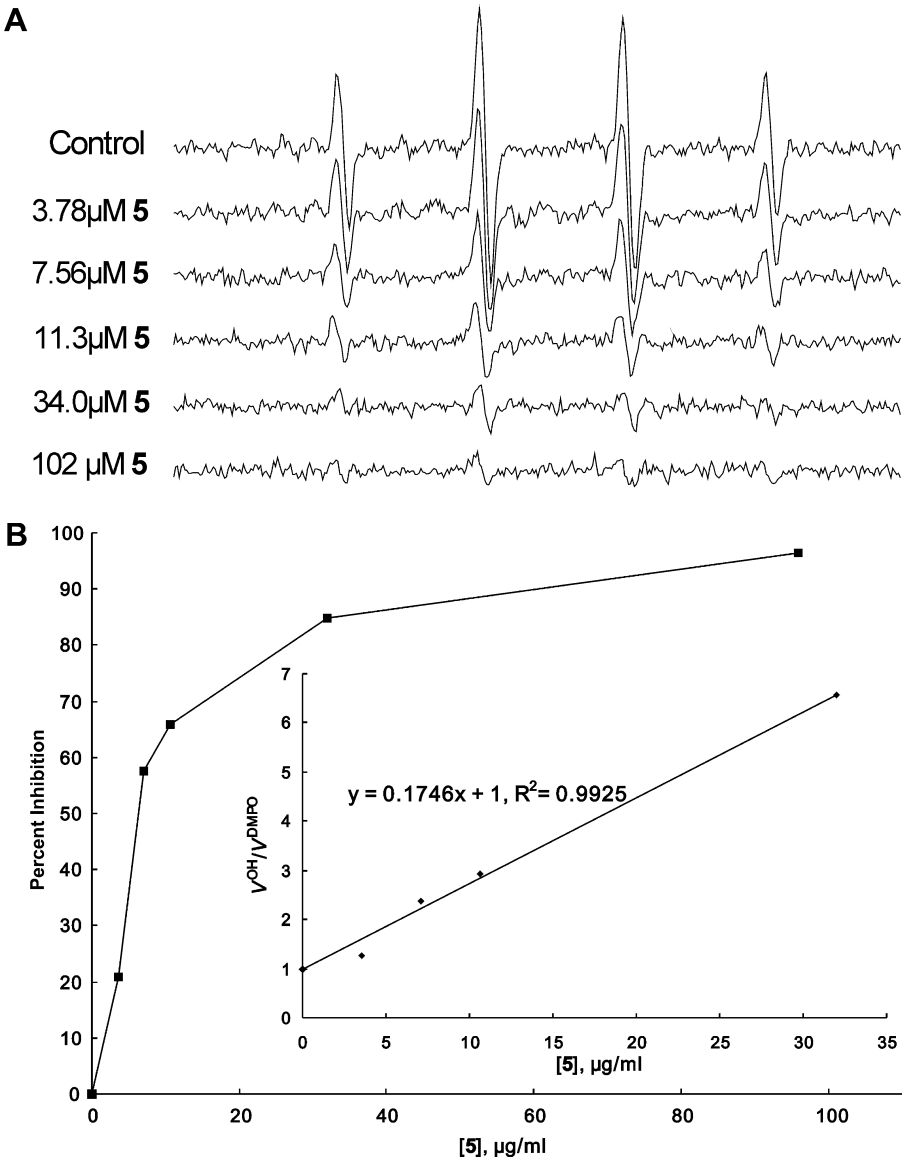

Fig. 2. Inhibitory effects of penta-*O*-galloyl-glucoside (**5**) on hydroxyl radical (·OH). (A) Effects of **5** on the generation of DMPO–OH adducts. (B) Percent inhibition calculated from the EPR signal intensities of the second peak present in A. Inset, plot of $V^{\cdot OH}/V^{DMPO}$ *versus* concentrations of **5**. $V^{\cdot OH}/V^{DMPO}$ is the ratio of the EPR signal intensities in the absence and presence of **5**, respectively.

0.9909 for **5**), the contents of predominant components **2** and **5** were quantified as 11.2% and 32.2% of MPE (w/w), respectively.

3.2. Antioxidant capacity

3.2.1. Hydroxyl radical (·OH)-scavenging activity

Hydroxyl radical (·OH) was produced by the Fenton reaction, where ferrous ions were oxidised and H_2O_2 was decomposed. As shown in Fig. 2A, a well-characterised 1:2:2:1 pattern of DMPO–OH with $a_N = a^H_B$ = 14.92 G was detected, consistent with the values in the reference (He et al., 2009). It has been reported that the EPR signals of DMPO–OH adducts were stable for several minutes, while in our work, it revealed that the signals declined with time (Fig. 3A, Control). Thus all the final EPR spectra should be recorded immediately after preparation. Addition of MPE, **2** or **5** into the detected systems inhibited the signal intensities in a concentration-dependent manner (Fig. 2A). The effective concentrations required to cause 50% inhibition of DMPO–OH adducts formation, namely IC_{50}, were evaluated to be 4.08 μg/ml for MPE, 35.6 μg/ml (0.18 mM) for **2**, and 5.31 μg/ml (5.65 μM) for **5**.

In order to measure the rate constants of antioxidants (A) with ·OH, the kinetic competition studies reported earlier (Naito et al., 1995) were adopted. According to the literature, three chemical equations could be established to illustrate the reaction mechanism:

$$Fe^{2+} + H_2O_2 \xrightarrow{k_O} Fe^{3+} + OH^- + \cdot OH \quad (1)$$

$$DMPO + \cdot OH \xrightarrow{k_D} DMPO{-}OH \quad (2)$$

and

$$A + \cdot OH \xrightarrow{k_A} \cdot A + H_2O \text{ or } HO{-}A \quad (3)$$

where Eqs. (1)–(3) represent the generation of ·OH, the reaction of DMPO with ·OH and the reaction of antioxidants with ·OH, respectively, with k_O, k_D, k_A as their individual rate constants. Here if

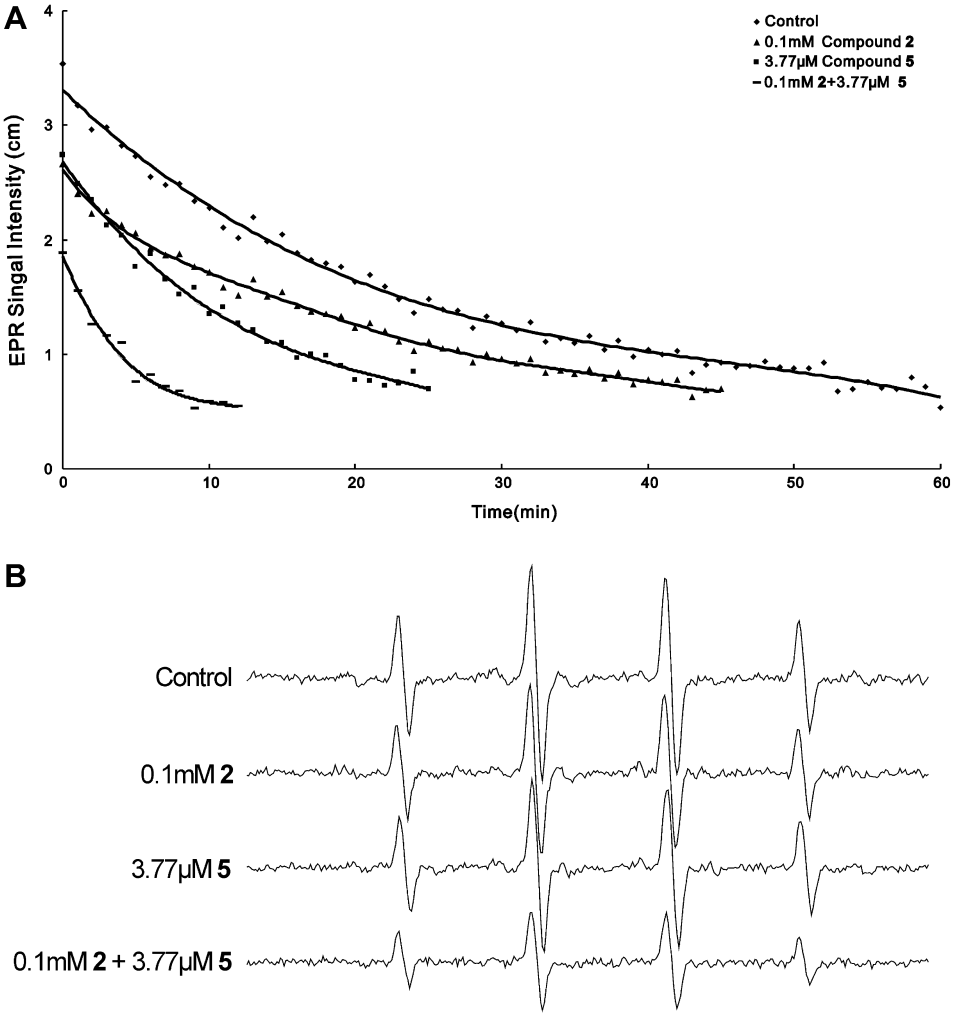

Fig. 3. Cooperation studies of ethyl gallate (**2**) and penta-*O*-galloyl-glucoside (**5**). (A) Scavenging effects of **2** and **5** at the indicated concentrations on the formation of DMPO–OH adducts with time. (B). 0.1 mM **2** and 3.77 μM **5** were, separately or together, added into the systems including 25 mM H_2O_2, 250 μM $FeSO_4$ and 50 mM purified DMPO.

concentrations of ferrous sulfate (Fe^{2+}), hydrogen peroxide (H_2O_2) and DMPO are fixed, the action of antioxidants against ·OH is only dependent on their concentrations alone.

Assuming that V^{OH}, V^{DMPO} and V^{A} represent the production velocities of ·OH, the combination velocities of ·OH with DMPO and the scavenging velocities of antioxidants, then,

$$V^{OH} = k_O[Fe^{2+}][H_2O_2] \quad (4)$$

$$V^{DMPO} = k_D[DMPO][\cdot OH] \quad (5)$$

$$V^{A} = k_A[A][\cdot OH] \quad (6)$$

Since competition between DMPO and antioxidants existed, another important equation could be obtained:

$$V^{OH} = V^{DMPO} + V^{A} \quad (7)$$

In addition, Eq. (5) can be transformed to Eq. (8):

$$[\cdot OH] = \frac{V^{DMPO}}{k_D[DMPO]} \quad (8)$$

Hence Eq. (6) could be written as:

$$V^{A} = \frac{k_A[A]V^{DMPO}}{k_D[DMPO]} \quad (9)$$

Substituting Eq. (9) into Eq. (7), Eq. (10) can be induced:

$$\frac{V^{OH}}{V^{DMPO}} = \frac{k_A[A]}{k_D[DMPO]} + 1 \quad (10)$$

where V^{OH}/V^{DMPO} can be measured as the ratio of EPR signal intensities in the absence and presence of antioxidants respectively. Obviously, under given conditions, a plot of V^{OH}/V^{DMPO} *versus* the concentration of antioxidants [A] presents a linear regression with k_A/k_D [DMPO] as its slope from which k_A can be calculated. Herein the reaction constant (k_D) between DMPO and ·OH is known (2.1×10^9; Finkelstein, Rosen, & Rauckman, 1980), and [DMPO] is fixed at 50 mM. As Fig. 2B inset shows, a line with a slope of 0.1746 ([**5**], μg/ml) was observed; therefore, k_A for **5** was 2.07×10^{15} M^{-1} S^{-1}. In the same way, k_A for **2** and MPE were calculated to be 1.65×10^{14} M^{-1} S^{-1} ([**2**], μg/ml) and 3.51×10^{15} M^{-1} S^{-1} ([MPE], μg/ml), respectively. Considering the individual IC_{50} values and rate constants, it demonstrated that MPE, **2** and **5** were potent hydroxyl radical scavengers ($k_A \gg k_D$) in the order: MPE > penta-*O*-galloyl-glucoside (**5**) > ethyl gallate (**2**).

Additionally, in order to observe how the EPR signal intensities change with increasing time, more experiments were carried out as presented in Fig. 3A, showing that all EPR signals declined with increasing time. During the initial periods, the signal reduction was fast and displayed a linear regression, then slowed down. The decrease of the signal intensities of the control was mainly attributed to the spontaneous regression of ·OH when the addition of the

scavengers and the spontaneous regression of ·OH were responsible for the quicker decrease of the other three systems. The line that is representative of 0.1 mM **2** and 3.77 μM **5** in the sample solution decreased most quickly and reached equilibrium in 13 min.

The reactions present in Fig. 4 were proposed (Yoshida et al., 1989) to illuminate the scavenging mechanism. Previous researchers reported that the existence of an *ortho*-dihydroxy structure in flavonoids was necessary for effective antioxidant activities as it confers high stability to the alkyl radical form and participates in electron delocalisation (Rice-Evans, Miller, & Paganga, 1996). This rule is also applicable for the gallate type compounds to support their potent capacities against ·OH. In addition, **5** having five galloyl groups possessed activity much stronger than that of **2** with only one galloyl group, partly demonstrating that the scavenging effects of the individual compounds in MPE increased with increasing number of galloyl groups in the molecule. Interestingly, the activity of **5** was 6.7 times not 5 times (weight to weight) more effective than that of **2**, which could be ascribed to the occurrence of intramolecular reactions in **5**. In general, intramolecular reactions occur more rapidly than corresponding intermolecular reactions, suggesting that **5,** with intramolecular reactions between two adjacent gallate molecules to generate some ellagitannins (Hatano et al., 1989), had a stronger inhibitory activity than **2**, which only underwent intermolecular reactions. Therefore, it could be hypothesised that compounds **6**, **7** and **9** with more gallate groups should show more powerful scavenging effects on ·OH than **5**.

Moreover, the synergistic effects of **2** and **5** may explain the strongest scavenging activity of MPE on ·OH. Ethyl gallate (**2**), actually, even at concentrations up to 0.1 mM did not significantly inhibit the formation of DMPO–OH adducts (Fig. 3B), while 3.77 μM penta-*O*-galloyl-glucoside (**5**) caused only 20.0% inhibition of EPR signal intensities (Fig. 3B). Compared to the control, a combination of 0.1 mM **2** and 3.77 μM **5** led to synergistic inhibition of about 55.7% (Fig. 3B). In the presence of the combination, the inhibitory effects of **2** and **5** were enhanced by factors of about 2.2 and 2.8, respectively. With increasing time, the EPR signals of the combination also decreased most quickly (Fig. 3A). Based on the reported explanation (Wrona, Korytowski, Rozanowska, Sarna, & Truscott, 2003), the prevention of **2** on **5** consumption by scavenging free radicals generated from the degradation of **5** resulted in more potent activity of **5** against ·OH, which could be a potential explanation for the synergistic effects.

3.2.2. Superoxide anion ($O_2^{\cdot-}$)-scavenging activity

Superoxide anions ($O_2^{\cdot-}$) generated in the photoirradiated riboflavin/EDTA systems were detected (a_N = 14.3 G, a_β^H = 11.7 G, a_γ^H = 1.3 G) as the spin adducts DMPO/$O_2^{\cdot-}$ (He et al., 2009). Herein 5.45 μg/ml MPE led to 69.8% inhibition of $O_2^{\cdot-}$ production (Fig. 5), indicating an effective scavenging activity of MPE on $O_2^{\cdot-}$. On the basis of the literature (Hatano et al., 1989), penta-*O*-galloyl-glucoside (**5**) exhibited a much strong inhibitory activity toward $O_2^{\cdot-}$ (IC_{50} = 3.4 μM), more potent than that of EGCG (IC_{50} = 31.6 μM), partially resulting in the powerful inhibition of MPE. Interestingly, in Fig. 5, some signals (•) characteristic of DMPO–OH adducts (1:2:2:1) were present in the spectrum of the reaction system with 5.45 μg/ml MPE. It might be owing to that ·OH generated from the reaction between H_2O_2 and $O_2^{\cdot-}$:

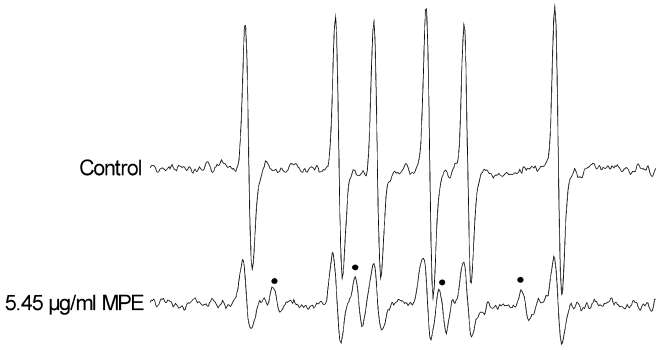

Fig. 5. Scavenging effect of MPE on superoxide anion ($O_2^{\cdot-}$). 0.3 mM riboflavin, 5.0 mM EDTA, 50 mM purified DMPO and 5.45 μg/ml MPE were photoirradiated by a UV lamp for 30 s and then the spectra were recorded immediately with UV light on. Some extra EPR signals were labelled to show their composition: DMPO–OH adducts (•, 1:2:2:1).

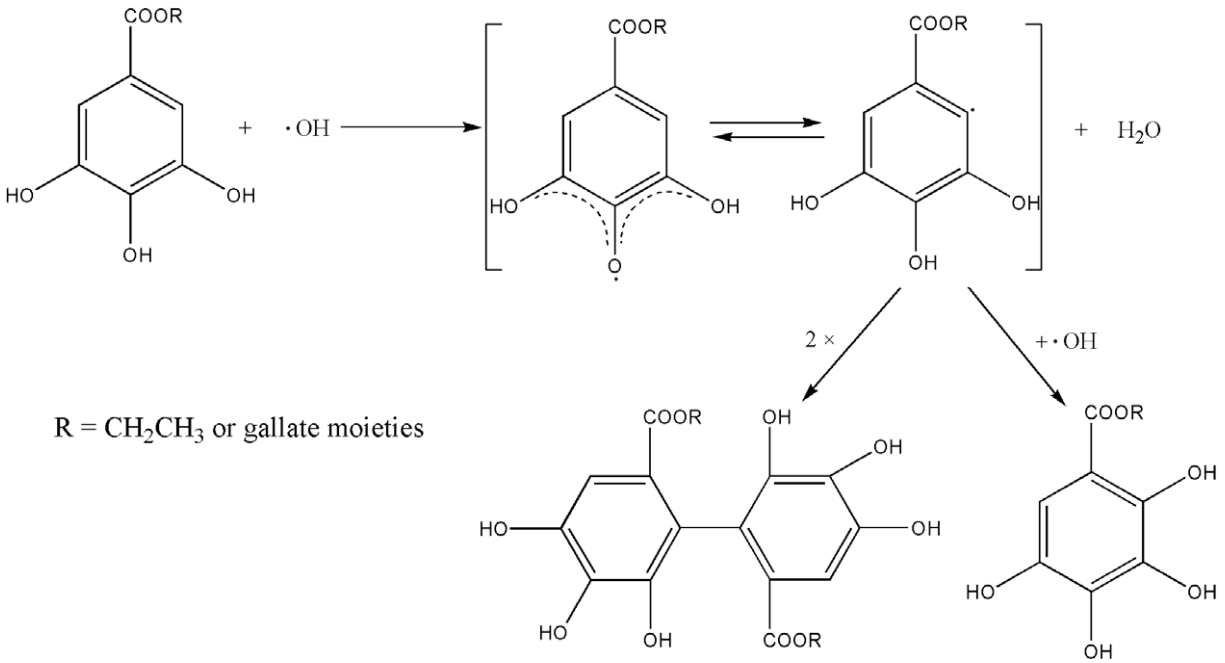

Fig. 4. Hypothetic mechanism of gallate type compounds against the generation of hydroxyl radical (·OH).

$$O_2^{\cdot-} + H_2O_2 \rightarrow O_2 + {\cdot}OH + OH^-$$

(Zang, Stone, & Pryor, 1995) were trapped by the redundant DMPO when the scavenger (MPE) reacted thoroughly. Here H_2O_2 was produced by the elimination of $O_2^{\cdot-}$ with MPE.

3.2.3. Singlet oxygen ($^1O_2$)-scavenging activity

Singlet oxygen ($^1O_2$) was formed by energy transfer from photo-excited rose Bengal to the molecular oxygen in the aqueous solution. TEMP, a spin trapper, reacted with $^1O_2$ to yield TEMP-$^1O_2$ adducts (TEMPO), showing characteristic EPR spectra (Fig. 6A, a^N = 17.2 G, g = 2.0056) with three equal intensity lines of nitroxide radicals (He et al., 2009). Fig. 6A exhibits the dose-dependent inhibition of **5** on TEMPO formation. Only 4.87 μg/ml MPE, 7.98 μg/ml **2** and 9.69 μg/ml **5** were required for 50% inhibition. Hence the three reactants, one of which was stronger than EGCG (IC_{50} = 6.64 μg/ml), have been proven to be capable of quenching $^1O_2$ *in vitro*; the order of efficacies was MPE > ethyl gallate (**2**) > penta-*O*-galloyl-glucoside (**5**). It should be noted that the order here is different from that observed in Section 3.2.1. It is appears more likely that these gallate type compounds quenched $^1O_2$ *via* a different mechanism from the one proposed in Fig. 4. However, the mechanism of gallate type compounds against $^1O_2$ remains unclear and requires future investigation.

Additionally, the kinetic model established in our previous work (He et al., 2009) was utilised to quantitatively evaluate the rate constants of the quenchers (Q) in aqueous systems. According to the literature, due to the competition between quenchers and TEMP, the final equation could be written as follows:

$$\frac{V^{^1O_2}}{V^{TEMP}} = \frac{k_Q[Q]}{k_{T[TEMP]} + k_d} + 1$$

When the chart of $V^{^1O_2}/V^{DMPO}$ *versus* the concentration of quenchers [Q] was drawn, a straight line with $k_Q/(k_T[TEMP] + k_d)$ as its slope was obtained (Fig. 6B inset). Here k_T, a known constant, and k_Q represent the rate constants for the reaction of $^1O_2$ with TEMP and quenchers (Q), respectively, and k_d is the decay rate of $^1O_2$. It is known that $k_d = 1/\tau$, where τ is the life time of $^1O_2$ in water (τ = 4.2 μs). As a result, k_Q could be calculated from the slope. Their individual quenching constants were found to be 1.98×10^{10} M^{-1} S^{-1} ([MPE], μg/ml), 1.64×10^{10} M^{-1} S^{-1} ([**2**], μg/ml),

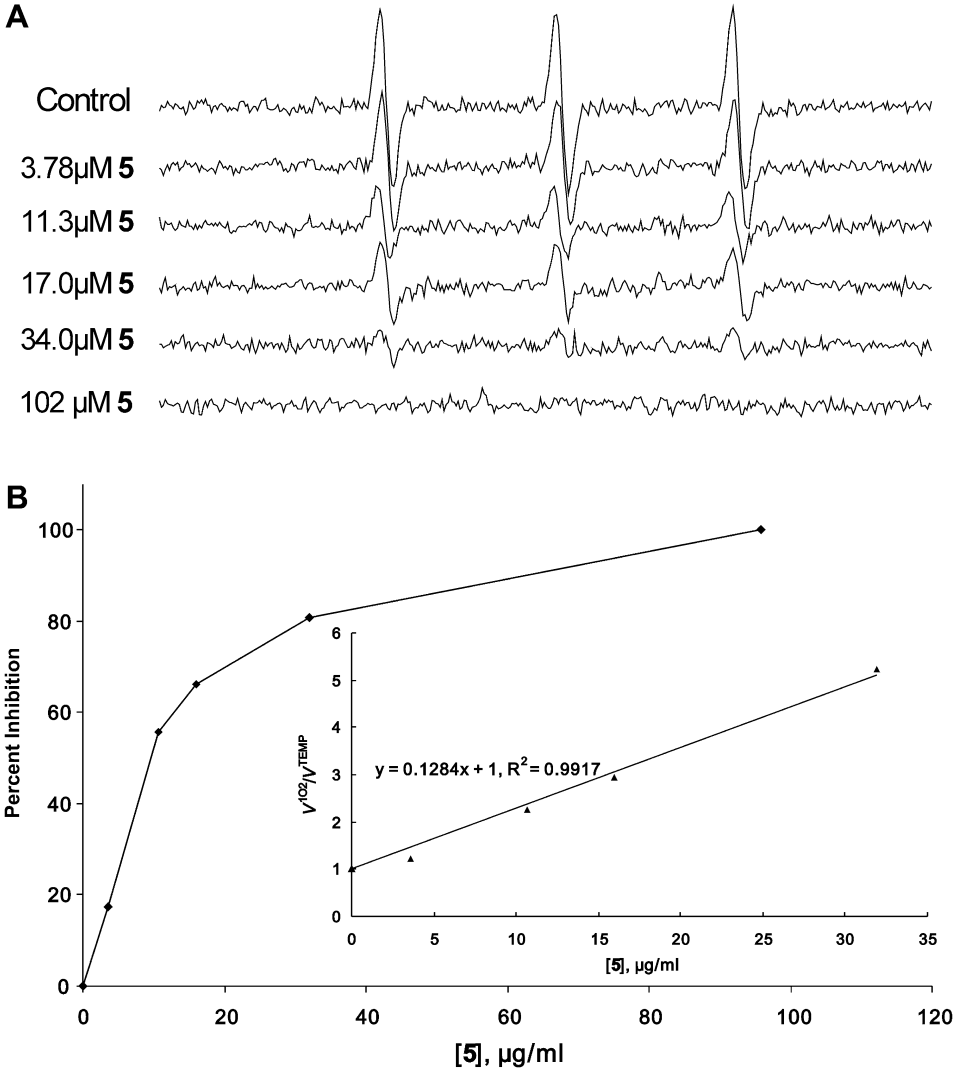

Fig. 6. Quenching effects of penta-*O*-galloyl-glucoside (**5**) on singlet oxygen ($^1O_2$). (A) Effects of **5** on the generation of TEMPO adducts. Samples, comprising 18 μM rose bengal, 23 mM TEMP and **5** at the indicated concentrations, were photoirradiated by a UV lamp for 2 min and then EPR spectra recorded instantly. (B) The EPR signal intensities of the first peak were selected to evaluate their corresponding scavenging inhibition. Inset plot of $V^{^1O_2}/V^{TEMP}$ *versus* various concentrations of **5**, where $V^{^1O_2}/V^{TEMP}$ represents the ratio of the EPR signal intensities in the absence and presence of **5**, respectively.

$1.42 \times 10^{10}\ M^{-1}\ S^{-1}$ ([**5**], μg/ml), demonstrating the effective capacities of the three quenchers ($k_Q \gg k_D$) as well as the same order as before: MPE > ethyl gallate (**2**) > penta-*O*-galloyl-glucoside (**5**).

4. Conclusions

In conclusion, bioassay-guided HPLC/ESI-MS^2 analysis was conducted to isolate two major valuable compounds, ethyl gallate (**2**) and penta-*O*-galloyl-glucoside (**5**), from the ethyl acetate extract of mango peels. Furthermore, using the highly sensitive and precise EPR spin-trapping technique, our present work indicated that ethyl acetate extract of mango peels (MPE) and two isolated compounds showed potent and unselective scavenging activities on ·OH, $O_2^{\cdot-}$ and $^1O_2$, three typical kinds of reactive oxygen species (ROS). Therefore mango peel waste could be reclaimed, not only resolving an environmental problem but also providing utilisation in both an experimental and clinical sense.

Acknowledgements

Financial support from NSFC of China (20772109) and Zhejiang Province (Z206150) is gratefully acknowledged.

References

Ajila, C. M., Bhat, S. G., & Rao, U. J. S. P. (2007). Valuable components of raw and ripe peels from two Indian mango varieties. *Food Chemistry, 102*, 1006–1011.

Barreto, J. C., Trevisan, M. T. S., Hull, W. E., Erben, G., Brito, E. S., Pfundstein, B., et al. (2008). Characterization and quantitation of polyphenolic compounds in bark, kernel, leaves, and peel of mango (*Mangifera indica* L.). *Journal of Agricultural and Food Chemistry, 56*, 5599–5610.

Beerh, O. P., Raghuramaiah, B., Krishnamurthy, G. V., & Giridhar, N. (1976). Utilization of mango waste: Recovery of juice from waste pulp and peel. *Journal of Food Science and Technology, 13*, 138–141.

Ćerković, G., Čanadanović-Brunet, J., Djilas, S., Savatović, S., Mandić, A., & Tumbas, V. (2008). Assessment of polyphenolic content and *in vitro* antiradical characteristics of apple pomace. *Food Chemistry, 109*, 340–347.

Eun-Jeon, P., Zhao, Y. Z., Ren-Bo, A., Youn-Chui, K., & Hwan, S. D. (2008). 1, 2, 3, 4, 6-penta-*O*-galloyl-β-D-glucose from Galla Rhois protects primary rat hepatocytes from necrosis and apoptosis. *Planta Medica, 74*, 1380–1383.

Finkelstein, E., Rosen, G. M., & Rauckman, E. J. (1980). Spin trapping kinetics of the reaction of superoxide and hydroxyl radicals with nitrones. *Journal of the American Chemical Society, 102*, 4994–4999.

Frenich, A. G., Torres, M. E. H., Vega, A. B., Vidal, J. L. M., & Bolaos, P. P. (2005). Determination of ascorbic acid and carotenoids in food commodities by liquid chromatography with mass spectrometry detection. *Journal of Agricultural and Food Chemistry, 53*, 7371–7376.

Haddock, E. A., Gupta, R. K., Al-Shafi, S. M. K., & Haslam, E. (1982). The metabolism of gallic acid and hexahydroxydiphenic acid in plants. Part 1. Introduction. Naturally occurring galloyl eaters. *Journal of the Chemical Society Perkin Transactions I*, 2515–2524.

Halliwell, B. B. (1974). Superoxide dismutase, catalase and glutathione peroxidase: Solution to the problems of living with oxygen. *New Phytologist, 105*, 1075–1086.

Hatano, T., Edamatsu, R., Hiramatsu, M., Mori, A., Fujita, Y., Yasuhara, T., et al. (1989). Effects of the interaction of tannins with co-existing substances. VI. Effects of tannins and related polyphenols on superoxide anion radical, and on 1, 1-diphenyl-2-picrylhydrazyl radical. *Chemical and Pharmaceutical Bulletin, 37*, 2016–2021.

He, S., Jiang, L. Y., Wu, B., Pan, Y. J., & Sun, C. R. (2009). Pallidol, a resveratrol dimer from red wine, is a selective singlet oxygen quencher. *Biochemical and Biophysical Research Communications, 379*, 283–287.

Ignarro, L. J., Balestrieri, M. L., & Napoli, C. (2007). Nutrition, physical activity, and cardiovascular disease: An update. *Cardiovascular Research, 73*, 326–340.

Lizarraga, D., Tourino, S., Reyes-Zutita, F. J., Kok, T. M. D., Delft, J. H. V., Mass, L. M., et al. (2008). Witch Hazel (*Hamamelis virginiana*) fractions and the importance of gallate moieties – Election transfer capacities in their antitumoral properties. *Journal of Agricultural and Food Chemistry, 56*, 11675–11682.

Mark, J. L. (1987). Oxygen free radicals linked to many diseases. *Science, 235*, 529–531.

Naito, Y., Yoshikazu, Y., Tanigawa, T., Sakurai, K., Yamasaki, K., Uchida, M., et al. (1995). Hydroxyl radical scavenging by rebamipide and related compounds: Electron paramagnetic resonance study. *Free Radical Biology and Medicine, 35*, 117–123.

Nishizawa, M., Yamagishi, T., Nonaka, G., Nishioka, I., Nagasawa, T., & Oura, H. (1983). Tannins and related compounds. XII. Isolation and characterization of galloylglucoses from Paeoniae radix and their effect on urea-nitrogen concentration in rat serum. *Chemical and Pharmaceutical Bulletin, 31*, 2593–2600.

Pastor, N., Weinstein, H., Jamison, E., & Brenowitz, M. (2000). A detailed interpretation of OH radical footprints in a TBP DNA complex reveals the role of dynamics in the mechanism of sequence specific binding. *Journal of Molecular Biology, 304*, 55–68.

Ravanat, J., Mascio, P. D., Martinez, G. R., Medeiros, M. H. G., & Cadet, J. (2000). Singlet oxygen induces oxidation of cellular DNA. *Journal of Biological Chemistry, 275*, 40601–40604.

Ribeiro, S. M. R., Barbosa, L. C. A., Queiroz, J. H., Knödler, M., & Schieber, A. (2008). Phenolic compounds and antioxidant capacity of Brazilian mango (*Mangifera indica* L.) varieties. *Food Chemistry, 110*, 620–626.

Rice-Evans, C. A., Miller, N. J., & Paganga, G. (1996). Structure–antioxidant activity relationships of flavonoids and phenolic acids. *Free Radical Biology and Medicine, 20*, 933–956.

Valko, M., Leibfritz, D., Moncol, J., Cronin, M. T. D., Mazur, M., & Telser, J. (2007). Free radicals and antioxidants in normal physiological functions and human disease. *The International Journal of Biochemistry and Cell Biology, 39*, 44–84.

Vile, G. F., & Tyrrell, R. M. (1995). Uva radiation-induced oxidative damage to lipids and proteins *in vitro* and in human skin fibroblasts is dependent on iron and singlet oxygen. *Free Radical Biology and Medicine, 18*, 721–730.

Wrona, M., Korytowski, W., Rozanowska, M., Sarna, T., & Truscott, T. T. (2003). Cooperation of antioxidants in protection against photosensitized oxidation. *Free Radical Biology and Medicine, 35*, 1319–1329.

Yoshida, T., Mori, K., Hatano, T., Okumura, T., Uehara, I., Komagoe, K., et al. (1989). Studies on inhibition mechanism of autoxidation by tannins and flavonoids. V. Radical-scavenging effects of tannins and related polyphenols on 1,1-diphenyl-2-picrylhydrazyl radical. *Chemical and Pharmaceutical Bulletin, 37*, 1919–1921.

Yu, L. L., Haley, S., Perret, J., & Harris, M. (2002). Free radical scavenging properties of wheat extracts. *Journal of Agricultural and Food Chemistry, 50*, 1619–1624.

Zang, L. Y., Stone, K., & Pryor, A. W. (1995). Detection of free radicals in aqueous extracts of cigarette tar by electron spin resonance. *Free Radical Biology and Medicine, 19*, 161–167.